

Biosensors

SPECIAL
ISSUE

A Fluorescent Probe with Aggregation-Induced Emission for Detecting Alkaline Phosphatase and Cell Imaging

Mingang Lin⁺, Jing Huang⁺, Fang Zeng,^{*} and Shuizhu Wu^{*[a]}

Abstract: Alkaline phosphatase (ALP) is associated with many diseases, and its accurate detection is of great significance. Fluorescent compounds with aggregation-induced emission (AIE) feature show beneficial advantages for serving as fluorescent probes. Herein, an AIE-active “turn on” probe for ALP detection was synthesized through incorporating a strong electron-withdrawing group (cyano) in the middle and the recognition moiety phosphate group at the end, thereby rendering a D–A–D structure with a relatively

high conjugation degree and good water solubility. It was found that the probe TPE-CN-pho is highly sensitive to ALP in aqueous solution. In the presence of ALP, the hydrophilic phosphate group on the probe is rapidly removed, resulting in a decrease in water solubility and subsequent formation of aggregates, thereby achieving aggregation-induced emission. Moreover, the probe TPE-CN-pho has also been successfully applied to imaging ALP in living cells.

Introduction

As an important member of the phosphatase family, alkaline phosphatase (ALP) can catalyze the hydrolysis of almost all phosphate monoesters to form inorganic phosphates and the corresponding alcohols, phenols, sugars and etc; and it can also catalyze the transfer reaction of phosphate groups.^[1] ALP plays an important role in phosphorylation and dephosphorylation of protein metabolism in cells. Previous researches indicate that the increase of endogenous ALP is closely related to the proliferation and differentiation of osteoblasts and bone mineralization.^[2,3] In addition, cumulative clinical manifestations indicate that abnormal increase of ALP in serum is associated with many diseases, such as breast cancer, prostate cancer, liver dysfunction, intestinal disease, bone disease, and diabetes.^[2–4] Thus examination of ALP activity/level could provide insight into how it works in a physiological environment and how it regulates treatment under pathological conditions. Thus, ALP has been included in the clinical routine tests.^[4]

Based on the enzyme’s ability of removing phosphate groups from a variety of materials, various methods have been used to study the expression levels and activities of ALP, such as electrochemistry, chromatography, colorimetric techniques and peptide microarrays.^[5–7] Although these methods can reflect the expression and activity of enzymes to some extent, they cannot be applied in living cells or organisms.^[6] Fluorescence imaging, as an highly sensitive, fast-response and efficient tool, can be used to track the state, changes, and activities of targets in cells or even some living organisms,^[8–15] thus it can be used for ALP dynamic detection. As for the fluorescent systems for detecting ALP, small-molecule fluorescent probes are favored because of their good chemical modification, biocompatibility and low cost.^[16,17]

Molecules with aggregation-induced emission (AIE) feature have beneficial advantages for serving as fluorescent probe.^[18–24] AIE fluorescent probes usually exhibit large Stokes shifts with almost no overlap between their excitation and emission spectra, which is conducive to fluorescence detection.^[25–28] Moreover, the AIE probes have better optical stability which is especially advantageous for long-time cell imaging and tracking.^[29] As for AIE probes, usually sufficient water solubility can ensure the probe’s good solubility in aqueous solution with almost no emission; while upon the probe’s reaction with the analyte, the resultant product has low water solubility, thus leading to aggregation with enhanced emission.^[19–29] At present, some AIE-active probes for ALP detection have been reported,^[30–37] for most of these probes, they are based on TPE molecule with relatively low conjugation degree, hence they usually require short excitation wavelength (e.g. UV light) and exhibit relatively short emission wavelength, which could erode the detection accuracy due to autofluorescence of biological samples (which usually involves blue emission). While in

[a] M. Lin,⁺ J. Huang,⁺ Prof. F. Zeng, Prof. S. Wu
State Key Laboratory of Luminescent Materials&Devices
College of Materials Science&Engineering
South China University of Technology
Guangzhou 510640 (China)
E-mail: mcfzeng@scut.edu.cn
shzhwu@scut.edu.cn

[⁺] These authors contributed equally to this work.

Supporting information and the ORCID identification number(s) for the author(s) of this article can be found under:
<https://doi.org/10.1002/asia.201801540>.

This manuscript is part of a special issue on aggregation-induced emission. A link to the Table of Contents of the special issue will appear here when the complete issue is published.

the case of AIE-active ALP probe, when the conjugation degree increases, one phosphate group can hardly provide enough water solubility to maintain the molecularly-dissolved state of probe molecules with no emission, and it's quite difficult to introduce multiple phosphate groups into one probe molecule and increase the conjugation degree at the same time. Therefore, to overcome this limitation, AIE probes for ALP detection with longer emission wavelength and new structure are highly sought-after.

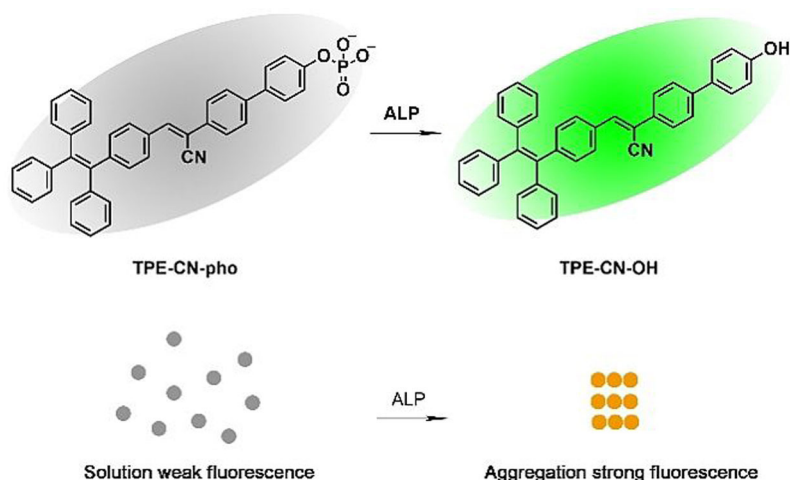
In this study, we designed a new fluorescent "turn-on" probe for ALP detection. The scaffold of the probe is based on the AIE-active fluorophore tetraphenylethene (TPE); through enhancing its conjugation degree as well as incorporating a strong electron-withdrawing group (cyano) in the middle and the hydrophilic recognition moiety phosphate group at the end, this D-A-D structure has longer excitation and emission wavelengths compared to TPE and in the meantime can maintain sufficient water solubility to quench fluorescence while extending conjugation length. The probe (TPE-CN-pho) shows quite good performance for ALP detection, and has longer excitation and emission wavelength compared with other TPE-based probes for ALP. The probe has quite good water solubility, and in the absence of ALP, the probe is almost non-emissive. While in the presence of ALP, phosphate group is removed from the probe molecule, correspondingly the probe turns into the enzymatic reaction product (with the same structure as TPE-CN-OH) which has low water solubility, and TPE-CN-OH molecules instantly form aggregates, subsequently strong green emission can be observed. Moreover, the probe has been successfully applied to imaging ALP in live cells.

Results and Discussion

Probe Synthesis and Detection Mechanism

The probe TPE-CN-pho was prepared via the synthetic route as shown in Scheme S1. The chemical structure of TPE-CN-pho was confirmed by NMR and Mass spectrometry (Figures S1–

S8). The probe TPE-CN-pho contains the ALP recognizing group—hydrophilic phosphate group at the end, which is the specific substrate of alkaline phosphatase. The probe shows almost no emission in water. When the probe reacts with ALP, the phosphate group is eliminated, which converts the phosphate group of the probe into hydroxyl group, and correspondingly the reaction product TPE-CN-OH is generated. Compared with TPE-CN-pho, TPE-CN-OH has poor solubility in water, and become strongly fluorescent due to the AIE feature, hence the detection of ALP can be achieved. To confirm the detection mechanism, the solution of the probe TPE-CN-pho before and after treatment with ALP for different time was investigated by HPLC (Figure 1c). Before being incubated with ALP, the peak for TPE-CN-pho can be observed at 2.07 min, and the peak for pure TPE-CN-OH is at 2.65 min; while after being incubated with ALP for 30 min, the peak for TPE-CN-pho at 2.07 min decreases and in the meantime that for TPE-CN-OH at 2.65 min appears. After being incubated with ALP for 60 min, only the peak for TPE-CN-OH can be observed. This result confirms the generation of TPE-CN-OH after the ALP-catalyzed reaction of TPE-CN-pho. The aggregation of TPE-CN-OH in buffer solution was confirmed by particle size analysis via dynamic light scattering (DLS) measurements (Figure 1a and 1b). As for TPE-CN-pho, particle size of around 10 nm can be observed (Figure 1a), while after reacting with ALP for 60 min larger aggregates with the size of about 100 nm can be observed as shown in Figure 1b, indicating the formation of aggregates from TPE-CN-OH molecules. The fluorescence spectra of pure TPE-CN-OH and the enzymatic reaction product were displayed in Figure 1d; by comparison, it is clear that the spectra are quite similar, indicating the enzymatic reaction product is actually TPE-CN-OH. The above results confirm that, the detection of ALP can be realized by TPE-CN-pho is due to the conversion of TPE-CN-pho into TPE-CN-OH, which aggregates in buffer solution, thereby resulting in aggregation-induced emission with enhanced green fluorescence.



Scheme 1. Illustration of the probe's response toward ALP, chemical structures of the probe TPE-CN-pho and the enzymatic reaction product TPE-CN-OH.

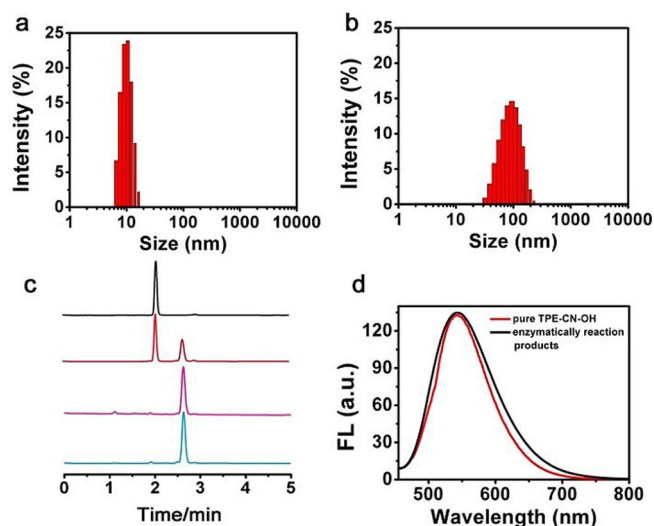


Figure 1. (a) Particle sizes measured by DLS for TPE-CN-pho ($10 \mu\text{M}$) without incubation with ALP. (b) Particle sizes measured by DLS, before collecting the DLS data, 60 minutes reaction of TPE-CN-pho and ALP at 37°C in Tris buffer (10 mM , $\text{pH } 8.0$) was carried out. (c) HPLC data for TPE-CN-pho and the reaction mixture of TPE-CN-pho and ALP at different incubation time. TPE-CN-pho without incubation with ALP (black); TPE-CN-pho ($10 \mu\text{M}$) + 200 U L^{-1} ALP after incubation for 30 min (red); TPE-CN-pho ($10 \mu\text{M}$) + 200 U L^{-1} ALP after incubation for 60 min (pink); pure TPE-CN-OH (blue). (d) Fluorescence spectra of pure TPE-CN-OH aggregates (red line) and enzymatically reacted product (black line) (in Tri-HCl buffer $\text{pH } 8.0$, containing $1\% \text{ DMSO}$). $\lambda_{\text{ex}} = 440 \text{ nm}$.

Fluorescence detection of ALP

First, absorption spectroscopy tests were conducted for TPE-CN-pho and TPE-CN-OH (Figure S9). The probe TPE-CN-pho shows absorption peak at around 375 nm , while TPE-CN-OH (the enzymatic reaction product) displays absorption peak at around 400 nm . Then we tested the AIE feature of the compound TPE-CN-OH. Figure 2a and 2b shows the aggregation-induced emission behavior of TPE-CN-OH in THF and water mixture solutions. When the volume ratio of water in the system is 80% or less, TPE-CN-OH is almost non-fluorescent because TPE-CN-OH has a high solubility in the system and fluorescence is quenched due to intramolecular rotation that dissipates the excited-state energy. When the volume ratio of water in the system is above 80% , the degree of aggregation of TPE-CN-OH increases due to its low solubility in water, and the solution emits strong fluorescence; and the higher the

water content, the greater the fluorescence intensity. TPE-CN-OH exhibits typical AIE feature. Figure 2c shows the fluorescence spectra of TPE-CN-pho and TPE-CN-OH in Tri-HCl buffer $\text{pH } 8.0$ (containing $1\% \text{ DMSO}$); it is clear that TPE-CN-OH aggregates exhibit obvious fluorescence compared with TPE-CN-pho.

Figure 3a shows the fluorescence spectra of the probe TPE-CN-pho ($10 \mu\text{M}$) in Tris buffer (10 mM , $\text{pH } 8.0$) at different time intervals after incubation with ALP (200 U L^{-1}). The fluorescence intensity of the solution is very weak in the absence of ALP. However, after incubation with ALP at 37°C , the fluorescence intensity of the solution increases. As the incubation time increases, the fluorescence intensity also increases. After incubating the TPE-CN-pho solution with ALP (200 U L^{-1}) for 60 min , the fluorescence intensity at 543 nm (Figure 3a) increases by about 9-fold. Figure 3c shows the fluorescence spectra of TPE-CN-pho in Tris buffer (10 mM , $\text{pH } 8.0$) after incubation for 60 min with different concentrations of ALP (0 – 200 U L^{-1}). As expected, TPE-CN-pho shows little fluorescence before addition of ALP. However, the fluorescence intensity increases after incubation with ALP. When the concentration of

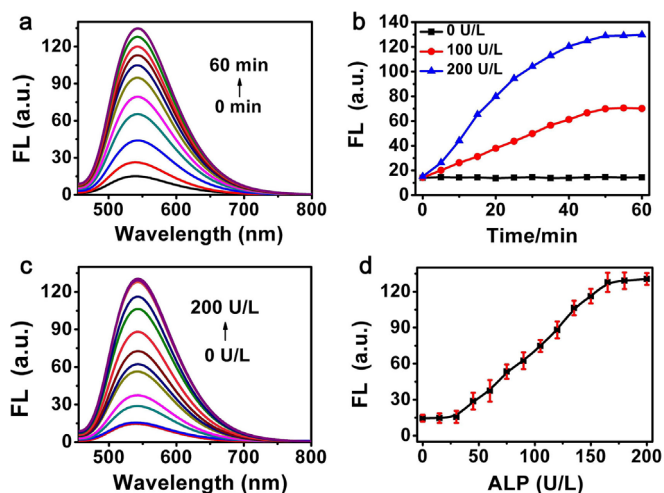


Figure 3. (a) Fluorescence spectra of TPE-CN-pho at different time intervals after incubation with ALP (200 U L^{-1}). $\lambda_{\text{ex}} = 440 \text{ nm}$. (b) Fluorescence intensity at 543 nm of TPE-CN-pho at different time intervals after incubation with different concentration of ALP ($0, 100, 200 \text{ U L}^{-1}$). (c) Fluorescence response of TPE-CN-pho ($10 \mu\text{M}$) upon the addition of different amounts of ALP: 0 U L^{-1} – 200 U L^{-1} . $\lambda_{\text{ex}} = 440 \text{ nm}$. (d) Fluorescence intensity at 543 nm upon the addition of different amounts of ALP: 0 U L^{-1} – 200 U L^{-1} .

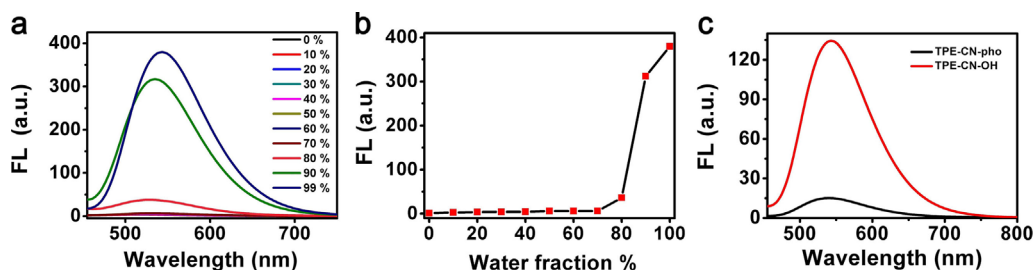


Figure 2. (a) Fluorescence spectra of TPE-CN-OH ($10 \mu\text{M}$) in THF/water mixture at different volume ratios of water (0% , 10% , 20% , 30% , 40% , 50% , 60% , 70% , 80% , 90% and 99%). (b) Fluorescence intensity at 543 nm at different volume ratios of water. $\lambda_{\text{ex}} = 400 \text{ nm}$. (c) Fluorescence spectra of pure TPE-CN-pho (black) and TPE-CN-OH (red) (in Tri-HCl buffer $\text{pH } 8.0$, containing $1\% \text{ DMSO}$) $\lambda_{\text{ex}} = 440 \text{ nm}$.

ALP is increased to 200 UL^{-1} , the fluorescence intensity at 543 nm increases by about 9 times. The detection limit is determined as 14.2 UL^{-1} (Figure S10). And the probe can function well in the pH range of 7.4–9.5 (Figure S11). These results indicate that TPE-CN-pho can effectively respond to ALP fluorescently.

It is known that ethylene-diaminetetraacetic acid (EDTA) can effectively inhibit the activity of ALP.^[37] To verify the specific recognition of ALP by the probe TPE-CN-pho, the inhibitor EDTA (0.5 mM) was incubated with ALP for 20 min and then incubated with the probe TPE-CN-pho for 60 min, afterwards fluorescence spectra were measured. It can be seen from Figure 4a that after incubating with EDTA the fluorescence of the probe is as weak as the untreated probe. While without the addition of EDTA, TPE-CN-pho with ALP treatment displays significant fluorescence emission. The result again confirms that the probe can respond towards ALP.

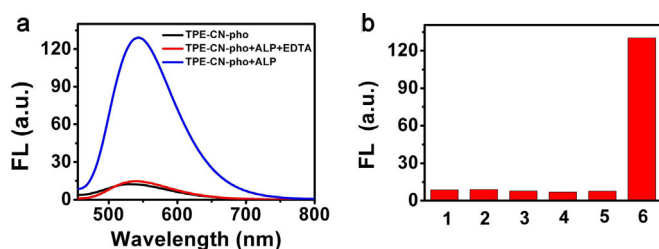


Figure 4. (a) Fluorescence spectra of $10 \mu\text{M}$ TPE-CN-pho alone (black), and TPE-CN-pho incubated with ALP (200 UL^{-1}) in the absence of EDTA (blue) and TPE-CN-pho incubated with ALP (200 UL^{-1}) in the presence of inhibitor EDTA (0.5 mM) (red) in Tris buffer. (b) Fluorescence response of TPE-CN-pho ($10 \mu\text{M}$) to various species: 1: Blank, 2: BSA (1 mg mL^{-1}), 3: Trypsin A (1 mg mL^{-1}), 4: ChE (200 UL^{-1}), 5: GOx (1 mg mL^{-1}) and 6: ALP (200 UL^{-1}). $\lambda_{\text{ex}} = 440 \text{ nm}$.

Previous studies demonstrated that, several enzymes such as esterase, pepsin and lysozyme won't affect the enzymatic reaction between ALP and the phosphate-containing substrates.^[17,31] Hence, in this study, the selectivity of the probe TPE-CN-pho for ALP detection was tested through incubation of the probe with some common biologically-relevant proteins such as BSA (bovine serum albumin), Trypsin, ChE (cholinesterase), GOx (glucose oxidase) under the same conditions. As shown in Figure 4b, TPE-CN-pho does not show fluorescence enhancement after incubation with these species. The good selectivity is due to the ability of ALP to specifically decompose the phosphate group in TPE-CN-pho.

Imaging ALP in Live Cells

We first examined cytotoxicity of TPE-CN-pho by using 3-(4,5-dimethyl-2-thiazolyl)-2,5-diphenyl-2H-tetrazolium bromide (MTT) assay. As shown in Figure S12, cell viabilities of HeLa cells (human cervical cancer cells), L929 cells (mouse aneuploid sarcoma cells) and HepG2 cells (human hepatocellular carcinoma cells) remain at high levels even when the TPE-CN-pho concentration is as high as $50 \mu\text{M}$, suggesting that TPE-CN-pho has good biocompatibility.

ALP is usually overexpressed in cancer cells, so TPE-CN-pho could be used for imaging ALP overexpressed cancer cells. In this experiment, HeLa, L929 and HepG2 cells were incubated with TPE-CN-pho; after washing once with PBS, the cells were directly imaged by using a fluorescence microscope. The fluorescence image of HeLa cells cultured with TPE-CN-pho shows green fluorescence, while the control group shows almost no fluorescence (Figure 5a). The occurrence of green fluorescence is attributed to the excess ALP in HeLa cells which cleaves the hydrophilic phosphate group from TPE-CN-pho thus generating TPE-CN-OH, and thereby emitting strong fluorescence upon aggregation. To further prove that the green fluorescence observed in HeLa cells was caused by ALP, the cells were incubated with the ALP inhibitor (levamisole hydrochloride) and the probe TPE-CN-pho; and it can be observed that the green fluorescence disappears. The results indicate that the intracellular fluorescence changes in HeLa cells are indeed caused by ALP. Moreover, we used the same method to image HepG2 cells and obtained similar results (Figure 5b). In contrast, L929 cells show no significant fluorescence changes after the addition of TPE-CN-pho because L929 does not overexpress ALP (Figure 5c). We suppose that the probes internalized by L929 cells do not undergo dephosphorylation due to the lack of ALP in the cells, which is in conformity with literature reports.^[38] These results indicate that TPE-CN-pho can be used as a fluorescent probe for detecting ALP and thereby imaging cancer cells.

Conclusions

A fluorescent “turn-on” probe for ALP detection was successfully developed with aggregation-induced emission feature through incorporating a strong electron-withdrawing group (cyano) in the middle and the recognition moiety phosphate group at the end, thereby rendering a D-A-D structure with relatively high conjugation degree and good water solubility and consequently longer-wavelength emission. After reaction with ALP, the probe TPE-CN-pho is converted to TPE-CN-OH with low water solubility. TPE-CN-OH readily aggregates and subsequently emits strong green fluorescence, thereby achieving ALP detection. Moreover, the probe TPE-CN-pho has good biocompatibility and has been successfully applied to cell imaging. Evidently, strong green fluorescence can be observed in HeLa cells and HepG2 cells after incubation with TPE-CN-pho because they overexpress ALP. In contrast, no fluorescence can be observed in L929 cells because they do not overexpress ALP. This study may provide useful insights into devising detection strategies for other enzymes.

Experimental Section

Materials: Unless otherwise specified, all solvents are purified and dried according to standard procedures. Phosphatase alkaline (ALP) from bovine intestinal mucosa and ethylenediaminetetraacetic acid disodium salt (EDTA) were purchased from Sigma Aldrich. Phosphate-buffered saline (PBS), dimethyl sulfoxide (DMSO) and MTT (3-[4,5-dimethylthiazol-2-yl]-2,5-diphenyltetrazolium bromide)

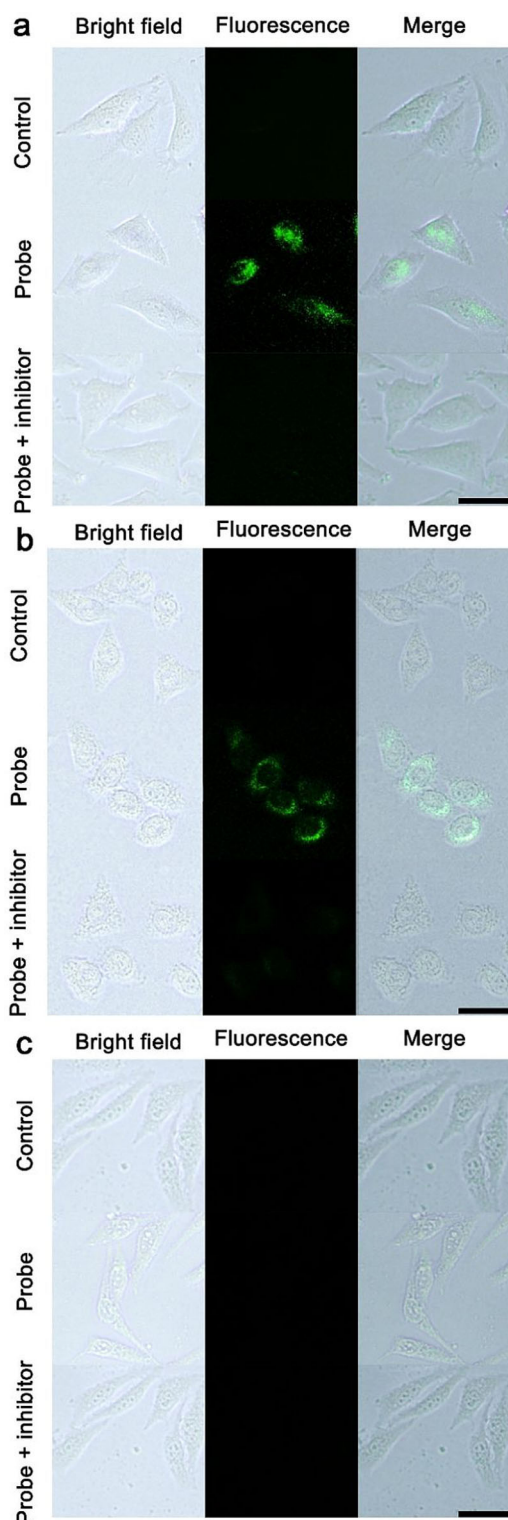


Figure 5. Bright field, fluorescence and merged image of HeLa cells (a), HepG2 cells (b) and L929 cells (c) that had been incubated with TPE-CN-pho (10 μM) or TPE-CN-pho (10 μM) + inhibitor (1 mM) at 37 $^{\circ}\text{C}$ for 60 min. Scale bar = 30 μm .

were obtained from Keygen Biotech. 1-Bromotriphenylethylene, (4-formylphenyl) boronic acid, tetrakis(triphenyl-phosphine) palladium, 4-bromophenylacetonitrile, (4-hydroxyphenyl) boronic acid, phosphorus oxychloride, ethyl acetate (EA), dichloro-methane

(DCM), ethanol (EtOH), petroleum ether (PE) and tetrahydrofuran (THF) were purchased from Aladdin. Other chemical reagents were commercially available and used as received.

Instrumentation: ^1H and ^{13}C NMR spectra were recorded on a Bruker Avance 600 MHz nuclear magnetic resonance spectrometer. Mass spectra were recorded on a Bruker LCQ DECA XP high performance liquid chromatography-mass spectrometer using the solvents of the chromatographic grade methanol and deionized water. Fluorescence spectra were recorded on a Hitachi F4600 fluorescence spectrometer. The quartz cells were selected to have a length and width of 1.0 cm. Absorption spectra and fluorescence spectra were recorded on a Hitachi U-3010 UV/Vis spectrophotometer and a Hitachi F-4600 Fluorescence Spectro-photometer. The quartz cells were selected to have a length and width of 1.0 cm. Fluorescence images were obtained using an Olympus IX 71 with a DP72 color CCD. The average size distribution and particle size of TPE-CN-pho and TPE-CN-OH solutions were determined by dynamic light scattering (DLS) with particle size analyzer (Malvern Zetasizer Nano-ZS90) at a fixed angle of 90 $^{\circ}$ at room temperature. HPLC analysis was determined on Agilent Technologies 1260 Infinity High Performance Liquid Chromatography. Methanol was used as eluents for all HPLC experiments. The flow rate was 1 mL min $^{-1}$.

Synthesis of TPE-CHO: 1-Bromotriphenylethylene (1005 mg, 3 mmol), (4-formylphenyl) boronic acid (675 mg, 4.5 mmol) and tetrakis (triphenylphosphine) palladium (73 mg, 0.09 mmol) were placed in a reaction flask. 20 mL of a mixed solution of 1,4-dioxane and 2 M potassium carbonate solution (v/v = 4:1) was added, and the system was vacuum-filled with nitrogen three times, and heated to 90 $^{\circ}\text{C}$, reacted for 24 h. After the reaction completed, the solvent was evaporated under reduced pressure and extracted with dichloromethane/water, and purified by silica gel column chromatography (petroleum ether: dichloromethane, v/v = 5:1, R_f = 0.3), to give a white solid, 80% yield. ^1H NMR (600 MHz, CDCl_3): δ = 9.90 (s, 1H), 7.61 (d, J = 8.2 Hz, 2H), 7.19 (d, J = 8.2 Hz, 2H), 7.13–7.09 (m, 9H), 7.04–6.99 ppm (m, 6H).

Synthesis of TPE-CN: The TPE-CHO (115.2 mg, 0.32 mmol) and 4-bromo-phenylacetonitrile (93.6 mg, 0.48 mmol) were put in a flask, and a solution of NaOH (13 mg, 0.32 mmol) in anhydrous ethanol (12 mL) was slowly added with stirring, and then reacting at room temperature for 3 h. After completion of the reaction, the solution was concentrated; the reaction flask was cooled in the refrigerator until there was precipitation. The reaction solution was filtered to obtain a precipitation solid, which was washed with ethanol and then dried in vacuum, to give a light yellow solid, yield 75%. ^1H NMR (600 MHz, CDCl_3): δ = 7.65 (d, J = 8.4 Hz, 2H), 7.57–7.52 (m, 2H), 7.51–7.47 (m, 2H), 7.39 (s, 1H), 7.15–7.09 (m, 11H), 7.07–7.01 ppm (m, 6H).

Synthesis of TPE-CN-OH: TPE-CN (268.5 mg, 0.5 mmol) obtained above, (4-hydroxyphenyl) boronic acid (69 mg, 0.5 mmol) and tetrakis (triphenylphosphine) palladium (40 mg, 0.04 mmol) were weighed in a reaction flask. 16 mL of a mixed solution of THF and 2 M potassium carbonate solution (v/v = 4:1) were added, and the system was vacuum-filled with nitrogen three times, and heated to 80 $^{\circ}\text{C}$, reacted for 24 h. After the reaction completed, the solvent was evaporated under reduced pressure and extracted with water/dichloromethane, and then purified by silica gel column chromatography (petroleum ether: dichloromethane, v/v = 1:2, R_f = 0.4), to give a green solid, 80% yield. ^1H NMR (600 MHz, CDCl_3): δ = 7.66 (dd, J = 8.5, 2.1 Hz, 4H), 7.58 (d, J = 8.5 Hz, 2H), 7.50–7.48 (m, 2H), 7.43 (s, 1H), 7.12 (ddt, J = 10.2, 6.1, 2.4 Hz, 12H), 7.06 (dd, J = 6.7, 3.0 Hz, 2H), 7.05–7.02 (m, 4H), 6.93–6.91 ppm (m, 2H).

Synthesis of TPE-CN-pho: TPE-CN-OH (275.6 mg, 0.5 mmol) was weighed into a reaction flask, and dissolved in anhydrous pyridine

(10 mL) and phosphorus oxychloride (0.466 mL, 5 mmol) was slowly added in reaction system in ice bath and stirred for 3 h. Ice cubes were then added to the reaction system and allowed to react overnight. After the reaction completed, the solvent was evaporated under reduced pressure, and then purified by silica gel column chromatography (dichloromethane: methanol, v/v = 10:1, $R_f = 0.3$), to give a yellow solid, 75% yield. $^1\text{H NMR}$ (600 MHz, DMSO): $\delta = 7.94$ (s, 1H), 7.74 (dt, $J = 12.4, 8.6$ Hz, 6H), 7.57 (d, $J = 8.6$ Hz, 2H), 7.19–7.10 (m, 11H), 7.05–6.98 (m, 6H), 6.88 ppm (t, $J = 5.7$ Hz, 2H). $^{13}\text{C NMR}$ (151 MHz, CDCl_3): $\delta = 155.61, 146.46, 143.36, 143.31, 143.19, 142.34, 141.42, 141.32, 140.04, 132.96, 132.67, 131.93, 131.70, 131.37, 131.32, 131.29, 128.75, 128.31, 127.91, 127.85, 127.68, 127.12, 126.90, 126.73, 126.69, 126.27, 118.16, 115.85, 110.23$ ppm. $^{31}\text{P NMR}$ (243 MHz, $[\text{D}_6]\text{DMSO}$): $\delta = -6.37$ ppm.

General procedure for the fluorescence measurement of TPE-CN-pho's response to ALP: All the measurements were performed in Tris buffer (10 mM, pH 8.0). As for the measurements involving different concentrations of ALP, TPE-CN-pho (20 μL , 1 mM in DMSO) was added to Tris buffer in a quartz cell (optical length: 1 cm), followed by different volumes of ALP. The concentration of ALP in each sample was 0–200 U L^{-1} . After incubation at 37 °C for 60 min, the fluorescence of the reaction solution was measured at $\lambda_{\text{ex}} = 440$ nm (slit widths: 5 nm). A control sample that contained no ALP was also prepared and measured under the same conditions. As for the measurements involving different incubation time, TPE-CN-pho (20 μL , 1 mM in DMSO) was added to Tris buffer in a quartz cell (optical length: 1 cm), followed by certain volume of ALP. After incubation at 37 °C for different time, the fluorescence of the reaction solution was measured at $\lambda_{\text{ex}} = 440$ nm (slit widths: 5 nm). A control sample that contained no ALP was also prepared and measured under the same conditions.

Cell culture: L929 cells (mouse aneuploid sarcoma cells) and HeLa cells (human cervical cancer cells) were cultured in DMEM supplemented adding 10% fetal bovine serum (FBS). HepG2 cells (Human hepatocellular carcinoma cells) were cultured in 1604 culture medium added with 10% fetal bovine serum (FBS). All the cells were grown at 37 °C, 5% CO_2 .

Cell viability assay: To assess the toxicity of the probe in living cells, the cells were treated with probe, and then cultured for 24 h. The toxicity of the probe to cells was determined by MTT according to ISO 10993-5. To reduce the errors in the measurement process, nine repeats were performed for each individual experiment, and the cell viability was estimated using statistical mean and standard deviation.

Fluorescence imaging of cells: For fluorescence imaging, cells were further incubated with TPE-CN-pho (10 μM) for 60 min at 37 °C under the corresponding conditions. A part of cells was incubated with the ALP inhibitor (levamisole hydrochloride, 1 mM) for 30 min, and then with the probe TPE-CN-pho (10 μM) for 60 min. After the completion of the incubation, the cells were washed once with PBS, and were directly imaged by using a fluorescence microscope.

General procedures for DLS and HPLC measurements: For the DLS experiment, 10 μM TPE-CN-pho (in Tri-HCl buffer pH 8.0, containing 1% DMSO) was first measured by particle size analyser (Malvern Zetasizer Nano-ZS90), then the TPE-CN-pho was treated with ALP (200 U L^{-1}) for 2 h at 37 °C, after enzymatic reaction, the resultant solution was again measured by particle size analyser. As for HPLC experiment, 10 μM TPE-CN-pho and 10 μM TPE-CN-OH in methanol were prepared. Additionally TPE-CN-pho (in Tri-HCl buffer pH 8.0, containing 1% DMSO) was treated with ALP (200 U L^{-1}) for 30 min and 60 min, respectively at 37 °C, and then the reaction solutions were added with diethyl ether, afterwards

the precipitates were re-dissolved in methanol for HPLC measurement. The above four solutions were tested with Agilent Technologies 1260 Infinity High Performance Liquid Chromatography with methanol as eluent and the flow rate was set as 1 min mL^{-1} .

Acknowledgements

This work was supported by NSFC (21788102, 21875069, 51673066 and 21574044) and the Natural Science Foundation of Guangdong Province (2016A030312002).

Conflict of interest

The authors declare no conflict of interest.

Keywords: aggregation-induced emission · alkaline phosphatase · biosensors · cell imaging · fluorescence · fluorescent probes

- [1] N. S. Fedarko, P. Bianco, U. Vetter, P. G. Robey, *J. Cell. Physiol.* **1990**, *144*, 115–121.
- [2] B. A. Rader, *Front. Immunol.* **2017**, *8*, 897.
- [3] a) M. J. Jedrzejewski, P. Setlow, *Chem. Rev.* **2001**, *101*, 607–618; b) F. Zheng, S. Guo, F. Zeng, J. Li, S. Wu, *Anal. Chem.* **2014**, *86*, 9873–9879.
- [4] A. Bernhard, L. Rosenbloom, *Proc. Soc. Exp. Biol. Med.* **1950**, *74*, 164–167.
- [5] C. Shen, X. Li, A. Rasooly, L. Guo, K. Zhang, M. Yang, *Biosens. Bioelectron.* **2016**, *85*, 220–225.
- [6] H. Sun, C. Lu, M. Uttamchandani, Y. Xia, Y. Liou, S. Yao, *Angew. Chem. Int. Ed.* **2008**, *47*, 1698–1702; *Angew. Chem.* **2008**, *120*, 1722–1726.
- [7] a) X. Li, X. Gao, W. Shi, H. Ma, *Chem. Rev.* **2014**, *114*, 590–659; b) J. Yan, S. Lee, A. Zhang, J. Yoon, *Chem. Soc. Rev.* **2018**, *47*, 6900–6916.
- [8] a) Y. Pak, S. Park, D. Wu, B. Cheon, H. Kim, J. Bouffard, J. Yoon, *Angew. Chem.* **2018**, *130*, 1583–1587; b) A. Kamkaewa, K. Burgess, *Chem. Commun.* **2015**, *51*, 10664–10667; c) C. Yu, X. Li, F. Zeng, F. Zeng, S. Wu, *Chem. Commun.* **2013**, *49*, 403–440.
- [9] a) H. Osaki, Ch. Chou, M. Taki, K. Welke, D. Yokogawa, S. Irlle, Y. Sato, T. Higashiyama, S. Saito, A. Fukazawa, S. Yamaguchi, *Angew. Chem. Int. Ed.* **2016**, *55*, 7131–7135; *Angew. Chem.* **2016**, *128*, 7247–7251; b) Y. Wu, J. Wang, F. Zeng, S. Huang, J. Huang, H. Xie, C. Yu, S. Wu, *ACS Appl. Mater. Interfaces* **2016**, *8*, 1511–1519; c) S. Fahs, P. Lujan, M. Köhn, *ACS Chem. Biol.* **2016**, *11*, 2944–2961; d) G. R. Casey, C. I. Stains, *Chem. Eur. J.* **2018**, *24*, 7810–7824.
- [10] a) K. Gu, Y. Xu, L. Hui, Z. Guo, S. Zhu, S. Zhu, P. T. D. James, H. Tian, W. Zhu, *J. Am. Chem. Soc.* **2016**, *138*, 5334–5340; b) A. C. Sedgwick, R. S. L. Chapman, J. E. Gardiner, L. R. Peacock, G. Kim, J. Yoon, S. D. Bull, T. D. James, *Chem. Commun.* **2017**, *53*, 10441–10443; c) Y. Huang, P. Zhang, M. Gao, F. Zeng, A. Qin, S. Wu, B. Z. Tang, *Chem. Commun.* **2016**, *52*, 7288–7291.
- [11] a) X. Chai, J. Xiao, M. Li, C. Wang, H. An, C. Li, Y. Li, D. Zhang, X. Cui, T. Wang, *Chem. Eur. J.* **2018**, *24*, 14506–14512; b) C. Yu, Y. Wu, F. Zeng, X. Li, J. Shi, S. Wu, *Biomacromolecules* **2013**, *14*, 4507–4514.
- [12] a) T. Schwarze, J. Riemer, H. Holdt, *Chem. Eur. J.* **2018**, *24*, 10116–10121; b) B. Ma, F. Zeng, F. Zeng, S. Wu, *Chem. Eur. J.* **2011**, *17*, 14844–14850; c) S. Shaw, W. Liu, C. Fernando, C. Schreiber, L. B. M. Mendiola, C. Zhai, F. M. Roland, S. J. Padanilam, B. D. Smith, *Chem. Eur. J.* **2018**, *24*, 13821–13829.
- [13] a) G. Ulrich, A. Sutter, M. Elhabiri, *Chem. Eur. J.* **2018**, *24*, 11119–11130; b) G. Wu, F. Zeng, S. Wu, *Anal. Methods* **2013**, *5*, 5589–5596; c) B. Ma, S. Wu, F. Zeng, Y. Luo, J. Zhao, Z. Tong, *Nanotechnology* **2010**, *21*, 195501; d) F. Zheng, F. Zeng, C. Yu, X. Hou, S. Wu, *Chem. Eur. J.* **2013**, *19*, 936–942.
- [14] a) X. You, L. Li, X. Li, H. Ma, G. Zhang, D. Zhang, *Chem. Asian J.* **2016**, *11*, 2918–2923; b) Y. Chen, X. Feng, Z. Sun, D. Wang, T. Yang, Z. Zhao, L. Li, X. Wang, H. Yu, *Chem. Asian J.* **2018**, *13*, 2781–2785; c) H. Feng, Q.

- Meng, Y. Wang, C. Duan, C. Wang, H. Jia, Zh. Zhang, R. Zhang, *Chem. Asian J.* **2018**, *13*, 2611–2618; d) M. Poddar, V. Sharma, S. M. Mobin, R. Misra, *Chem. Asian J.* **2018**, *13*, 2881–2890; e) D. Soni, N. Duvva, D. Badgurjar, T. K. Roy, S. Nimesh, G. Arya, L. Giribabu, R. Chitta, *Chem. Asian J.* **2018**, *13*, 1594–1608.
- [15] a) Y. Wu, S. Huang, J. Wang, L. Sun, F. Zeng, S. Wu, *Nat. Commun.* **2018**, *9*, 3983; b) R. Takagi, A. Takeda, D. Takahashi, K. Toshima, *Chem. Asian J.* **2017**, *12*, 2656–2659; c) A. Pramanik, S. R. Chavva, B. Priya, V. Nellore, K. May, T. Matthew, S. Jones, A. Vangara, P. C. Ray, *Chem. Asian J.* **2017**, *12*, 665–672.
- [16] S. Li, C. Li, Y. Li, J. Fei, P. Wu, B. Yang, J. Yang, S. Nie, *Anal. Chem.* **2017**, *89*, 6854–6860.
- [17] H. Zhang, C. Xu, J. Liu, X. Li, L. Guo, X. Li, *Chem. Commun.* **2015**, *51*, 7031–7034.
- [18] J. Mei, N. Leung, R. T. K. Kwok, J. Lam, B. Z. Tang, *Chem. Rev.* **2015**, *115*, 11718–11940.
- [19] D. Wang, L. Michelle, G. Shan, R. T. K. Kwok, J. Lam, H. Su, Y. Cai, B. Z. Tang, *Adv. Mater.* **2018**, *30*, 1802105.
- [20] Z. Zheng, T. Zhang, H. Liu, Y. Chen, R. T. K. Kwok, C. Ma, P. Zhang, H. H. Y. Sung, I. D. Williams, J. Lam, K. S. Wong, B. Z. Tang, *ACS Nano* **2018**, *12*, 8145–8159.
- [21] M. Li, Y. Gao, Y. Yuan, Y. Wu, Z. Song, B. Z. Tang, B. Liu, Q. Zheng, *ACS Nano* **2017**, *11*, 3922–3932.
- [22] W. Wu, D. Mao, H. Fang, S. Xu, C. Chao, J. Zhang, X. Cheng, Y. Yuan, D. Ding, D. Kong, B. Liu, *Adv. Mater.* **2017**, *29*, 1700548.
- [23] F. Hu, D. Mao, Kenry, X. Cai, W. Wu, D. Kong, B. Liu, *Angew. Chem.* **2018**, *130*, 10339–10343.
- [24] Y. Hang, J. Wang, T. Jiang, N. Lu, J. Hua, *Anal. Chem.* **2016**, *88*, 1696–1703.
- [25] L. Zong, H. Zhang, Y. Li, Y. Gong, D. Li, J. Wang, Z. Wang, Y. Xie, M. Han, Q. Peng, X. Li, J. Dong, J. Qian, Q. Li, L. Zhen, *ACS Nano* **2018**, *12*, 9532–9540.
- [26] F. Guo, W. Gai, Y. Hong, B. Z. Tang, J. Qin, Y. Tang, *Chem. Commun.* **2015**, *51*, 17257–17260.
- [27] X. Dong, F. Hu, Z. Liu, G. Zhang, D. Zhang, *Chem. Commun.* **2015**, *51*, 3892–3895.
- [28] Y. Zhao, R. T. K. Kwok, J. Lam, B. Z. Tang, *Nanoscale* **2016**, *8*, 12520–12523.
- [29] Z. Song, Y. Zhao, R. T. K. Kwok, J. Lam, B. Liu, B. Z. Tang, *ACS Appl. Mater. Interfaces* **2014**, *6*, 17245.
- [30] J. Liang, R. T. K. Kwok, H. Shi, B. Z. Tang, B. Liu, *ACS Appl. Mater. Interfaces* **2013**, *5*, 8784–8789.
- [31] F. Cao, Y. Long, S. Wang, B. Li, J. Fan, X. Zeng, *J. Mater. Chem. B* **2016**, *4*, 4534–4541.
- [32] X. Gu, G. Zhang, Z. Wang, W. Liu, L. Xiao, D. Zhang, *Analyst* **2013**, *138*, 2427–2431.
- [33] H. Liu, K. Li, X. Hu, L. Zhu, Q. Rong, Y. Liu, X. Zhang, F. Qu, W. Tan, *Angew. Chem. Int. Ed.* **2017**, *56*, 11788–11792; *Angew. Chem.* **2017**, *129*, 11950–11954.
- [34] W. Zhang, H. Yang, N. Li, N. Zhao, *RSC Adv.* **2018**, *8*, 14995–15000.
- [35] Q. Chen, N. Bian, C. Cao, X. Qiu, A. Qi, B. Han, *Chem. Commun.* **2010**, *46*, 4067–4069.
- [36] L. Zhao, S. Xie, X. Song, J. Wei, Z. Zhang, X. Li, *Biosens. Bioelectron.* **2017**, *91*, 217–224.
- [37] R. L. Dean, *Biochem. Mol. Biol. Educ.* **2002**, *30*, 401–407.
- [38] a) H. Liu, Z. Lv, K. Ding, X. Liu, L. Yuan, H. Chen, X. Li, *J. Mater. Chem. B* **2013**, *1*, 5550–5556; b) X. Hou, Q. Yu, F. Zeng, J. Ye, S. Wu, *J. Mater. Chem. B* **2015**, *3*, 1042–1048.

Manuscript received: October 18, 2018

Revised manuscript received: November 13, 2018

Accepted manuscript online: ■ ■ ■ ■, 0000

Version of record online: ■ ■ ■ ■, 0000

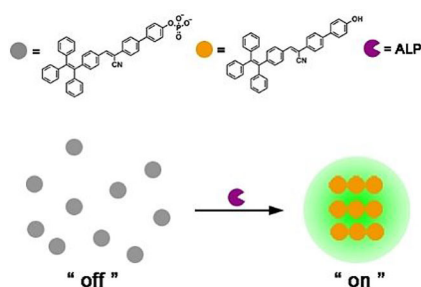
FULL PAPER

Biosensors

Mingang Lin, Jing Huang, Fang Zeng,*
Shuizhu Wu*



**A Fluorescent Probe with
Aggregation-Induced Emission for
Detecting Alkaline Phosphatase and
Cell Imaging**



The joy of being a DAD: An AIE-active "turn-on" probe, TPE-CN-pho, for alkaline phosphatase (ALP) detection has been developed with a donor-acceptor-donor (D-A-D) structure, in which phosphate acts as both the recognition moiety and hydrophilic moiety. The probe has been successfully applied in detecting ALP in aqueous media as well as imaging ALP in living cells.